Optical reflectance anisotropy of buried Fe nanostructures on vicinal W(110)

K Fleischer, L Carroll, C Smith and J F McGilp[1]

School of Physics, Trinity College Dublin, Dublin 2, Republic of Ireland

Abstract
The optical anisotropy of Au protected Fe layers grown on a vicinal W(110) surface has been investigated using reflectance anisotropy spectroscopy (RAS). Iron nanostripes formed at submonolayer coverage, as well as Fe layers up to 3 ML coverage, were protected by 12 and 16 nm gold caps and measured *ex situ* under ambient conditions. The RAS is dominated by structures originating in the interfacial W(110) region, modified by the absorption in the Au cap and possibly by uniaxial strain in the Au cap itself. The Fe nanostructures themselves do not produce a significant RAS signature but, nevertheless, differences with Fe coverage were identified and explained in terms of a simple isotropic Fe absorbing layer, together with strain relief in the W/Fe/Au interfacial region.

(Some figures in this article are in colour only in the electronic version)

1. Introduction

Laterally confined nanostructures are attracting considerable interest due to their unusual physics and potential technological applications. However, to be useful, the nanostructures have to be protected from environmental corrosion and contamination and this generally necessitates capping the structure with a thin protecting layer. The buried interfacial region of such a capped structure is not amenable to conventional surface science techniques, including scanning probe methods. Epioptic techniques, such as reflection anisotropy spectroscopy (RAS) and optical second-harmonic generation (SHG), offer the possibility of exploring the buried interfacial region through such thin capping layers [1]. Magnetic interfaces can also be explored, using techniques like magnetic SHG (MSHG) [2], and magnetic nanostructures are being investigated as advanced materials for sensors, actuators and magnetic data storage [3].

The W(110)/Fe system has proved to be a very useful model system for studying low dimensional magnetism. Pseudomorphic Fe layers grown on singular W(110) surface were studied in the late eighties [4, 5], and in the last 10 years these studies have been extended to

---

[1] Author to whom any correspondence should be addressed.

vicinal W(110) substrates [6–10]. The growth mode of Fe on the vicinal W(110) crystal, offcut by about 1° towards [100], is well understood. The substrate has regularly spaced single height atomic steps running in the [001] direction, separated by well ordered terraces approximately 40 atoms wide. For submonolayer coverage of Fe, room temperature deposition followed by annealing produces a monolayer stripe structure, nucleated at the step edges, and with a width dependent on the coverage [7]. For integer monolayer coverage, the basic structure of 1, 2 and 3 ML films is pseudomorphic monolayer, bilayer and then monolayer + island. A Stranski–Krastanov growth mode has been established by 3 ML Fe coverage, with large, flat islands, typically a few hundred nanometres long by about 10 atomic layers in height, sitting on a pseudomorphic Fe monolayer [11]. In this paper the optical anisotropy of this model W(110)/Fe system, on capping by Au, is investigated. These capped structures have shown magnetic behaviour even after several months of exposure to the ambient [12].

2. Experiment

The samples were prepared under ultrahigh vacuum (UHV) conditions with a base pressure below 4×10^{-11} mbar. The vicinal W(110) single crystal, offcut 1.4° in the [$1\bar{1}0$] direction, was cleaned by thermal cycling in 5×10^{-8} mbar of O_2 and then flashing to 2200 K until a sharp (1×1) low energy electron diffraction (LEED) pattern appeared and no residual C and O contamination was observed with Auger electron spectroscopy (AES). Iron was evaporated onto the clean W(110) surface at room temperature, using an electron beam evaporator, the deposition rate having been calibrated using AES. The background pressure remained below 3×10^{-10} mbar during Fe deposition. AES showed no detectable contamination of the Fe layers at the end of the deposition process. The sample was then annealed for 5 min at 800 K to produce well ordered Fe nanostructures, as revealed by LEED, and in agreement with previous work [6, 8]. An eclipsing mask was used during deposition to produce a checkerboard pattern of 4 patches with 0, 1, 2, and 3 ML Fe for the integer monolayer measurements and 0, 0.25, 0.5, and 0.75 ML for the submonolayer study. Thirty to forty ML (12–16 nm) of Au were deposited from a commercial high temperature Knudsen cell onto the substrate at room temperature (RT), where no interdiffusion of Au occurs [9]. The pressure remained below 1×10^{-10} mbar during this final step. LEED showed no crystalline order at the Au surface after the RT deposition.

Capped samples can only be investigated by optical techniques such as RAS or SHG if the buried interfacial region is still accessible to the incident light. As the penetration of light into metals in the visible region is small, the capping layer thickness is a compromise between access to the buried interface and protection from corrosion and contamination by the ambient. Earlier experiments using 18 ML of Ag were unsuccessful in protecting the Fe/W(110) interface, due to the reaction of the Ag layer with sulphur from the ambient [13]. Gold layers of about 30 ML thickness have proved to be a successful compromise. The thickness is comparable to the penetration depth (defined as the depth at which the intensity inside the material has fallen to $1/e$ of its incident value) at the laser spectral energy of 1.55 eV used for SHG measurements. For the RAS measurements, which cover a spectral range of 1.5– 5 eV, the penetration depth varies from 11 to 18 nm, which will affect the measured line shape of the RAS spectra of capped W(110)/Fe. The interpretation of the energies and amplitudes of RAS structures, and the comparison with uncapped samples, is thus not straightforward and model calculations of the dielectric response of the system are required. The bulk dielectric function of tungsten is well known, but the dielectric function of ultrathin Au layers can vary considerably from that of bulk Au [14]. Variable angle spectroscopic ellipsometry (VASE) measurements of the capped samples were used to determine the dielectric response of the Au capping layer. The use of an accurate thin film gold dielectric function is crucial for determining

of the anisotropic oscillator parameters for the RAS spectra, as the capping layer distorts the measured anisotropy of the interfacial region.

The RAS system is of conventional design [15], and uses two calcite polarizers, a quartz photoelastic modulator and a photomultiplier. The reflectance anisotropy of the whole sample is measured:

$$\frac{\Delta \tilde{r}}{\tilde{r}} = 2\frac{\tilde{r}_{[001]} - \tilde{r}_{[1\bar{1}0]}}{\tilde{r}_{[001]} + \tilde{r}_{[1\bar{1}0]}} \tag{1}$$

where $\tilde{r}$ denotes the complex Fresnel reflectivity [16]. The direction parallel to the steps ([001]) is defined as x, and the orthogonal direction ([1$\bar{1}$0]) as y. There are no *ab initio* calculations of the optical response of the W(110)/Fe/Au system and so the measurements are compared with simpler optical models using the known or measured dielectric functions. The normal incidence reflectance, R, of a five phase model, comprising bulk, damped anisotropic harmonic oscillator, Fe structure, Au capping layer and ambient, for the [001] and [1$\bar{1}$0] axes is calculated and then related to the complex reflectivity using $\Delta R/R \approx 2\Delta\tilde{r}/\tilde{r}$. Of the various phases, only the oscillator, introduced to model the W(110) anisotropic surface and interface states, and the submonolayer Fe structures, would be expected to show significant optical anisotropy. The real and imaginary part of the dielectric response of the anisotropic oscillator in direction i, with eigenfrequency $\omega_{0,i}$, is given by:

$$\varepsilon_{1,i} = \frac{A_i(\omega_{0,i}^2 - \omega^2)}{(\omega_{0,i}^2 - \omega^2)^2 + \Gamma_i^2\omega^2}, \qquad \varepsilon_{2,i} = \frac{A_i\Gamma_i\omega}{(\omega_{0,i}^2 - \omega^2)^2 + \Gamma_i^2\omega^2} \tag{2}$$

where the amplitude A_i is proportional to the oscillator strength and Γ_i the damping which corresponds to the full width at half maximum height (FWHM) of the peaklike structure in ε_2. In the region around $\omega_{0,i}$ this is equivalent to the Lorentz oscillator used in [16]. It has been shown that, for semiconductor multilayers, deconvolution of the surface and interface contributions is possible using such models [18]. The tabulated bulk dielectric functions for Au and W [17], and for Fe [19] were used, together with the dielectric function of the Au capping layer determined from the VASE measurements. There are a maximum of 6 parameters ($\omega_{0,i}, A_i$ and Γ_i, for $i = x, y$) that can be adjusted to give optimal values by least squares fitting to the measured RAS response. It should be noted that RAS measures $\Delta\varepsilon d$ and the anisotropic oscillator strengths throughout refer to an assumed thickness, d, of 3 Å for the interfacial region.

3. Integer monolayers of Fe and comparison with the uncapped surface

The effect of Au capping on the RAS spectra of the clean vicinal W(110) surface is shown in figure 2(a), with the singular surface results of Martin *et al* [20] for comparison. The clean surface shows an oscillatory structure around 3.4 eV which becomes sharper and less dispersive in shape on capping with Au. There is also a significant difference between the clean singular and vicinal W(110) spectra. As has been discussed previously for this vicinal surface [13], the broad, negative contribution above 4 eV is in the same spectral region as the step contributions from Cu(111) [21] and Au(110) surfaces [22]. This structure is rapidly quenched on adsorption [13]. It is also possible that anisotropic, optical scale, changes in the surface morphology arising from the cleaning procedure contribute to the line shape in this spectral region.

The main interest lies in the feature around 3.4 eV. Martin *et al* attributed this to a transition from an occupied p-band surface state about 1 eV below the Fermi level to unoccupied d-band states of the W(110) surface [20]. The general similarity of the RAS response of the clean and adsorbate covered surface in this spectral region may indicate that such a transition still occurs,

3
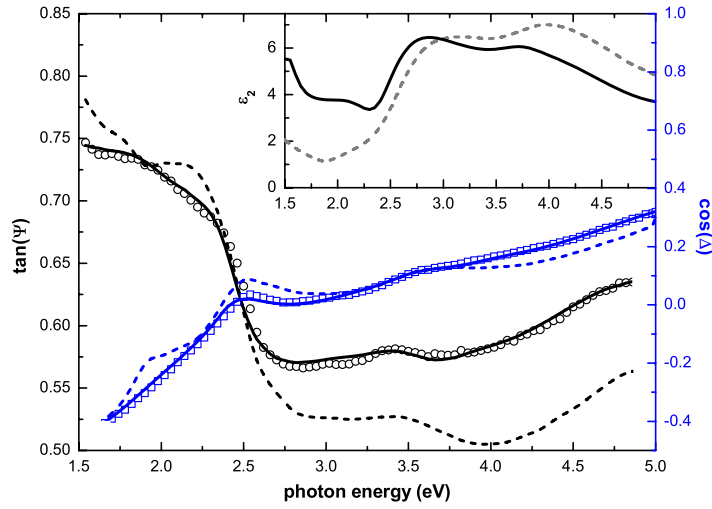
Figure 1. Spectroscopic ellipsometry measurements of the capped Au capped W(110) (tan ψ: $\circ$, cos Δ: $\square$). The solid and dashed lines show least square fits to the raw data using the thin film Au dielectric function and the known bulk values [17], respectively, for one angle of incidence. The inset compares the imaginary parts of the thin film dielectric function (——) directly to literature data (– – –) [17].

Table 1. Numerical values for least square fits of the anisotropic oscillator parameters. The confidence interval of the fits is given for all free parameters. Parameters fixed for all fits are the thickness d of the oscillator layer (3 Å), the dielectric functions for W and Fe (taken from [17] and [19]), and the thin film Au dielectric function and thickness derived from the VASE measurements (see figure 1). Numbers in italics were kept fixed in a particular fit.

	A_x (eV^2)	$\omega_{0,x}$ (eV)	Γ_x (eV)	A_y (eV^2)	$\omega_{0,y}$ (eV)	Γ_y (eV)	Comment	χ^2
W(110) (see figure 2)								
W(110) [20]	*150*	3.0 ± 0.1	1.9 ± 0.3	*150*	3.3 ± 0.1	1.6 ± 0.2	Fixed A (0 ML fit)	2.6
Au/W(110) (see figure 2)								
0 ML	150 ± 40	3.5 ± 0.1	0.8 ± 0.1	A_x	3.6 ± 0.1	Γ_x	Equal A and Γ	1.45
	150 ± 80	3.4 ± 0.3	0.8 ± 0.2	150 ± 80	3.5 ± 0.3	0.8 ± 0.1	Fully anisotropic	1.44
Au/Fe/W(110) (see figures 2 and 3)								
1 ML	Fixed values of 0 ML equal A and Γ fit, *3* Å Fe layer							3.4
	150	3.42 ± 0.05	*0.8*	A_x	3.49 ± 0.05	Γ_x	A and Γ (0 ML fit)	2.9
	150 ± 40	3.5 ± 0.1	0.8 ± 0.1	A_x	3.5 ± 0.1	Γ_x	Equal A and Γ	2.8
	130 ± 80	3.4 ± 0.1	0.7 ± 0.2	150 ± 80	3.5 ± 0.1	0.8 ± 0.2	Fully anisotropic	1.38
2 ML	Fixed values of 1 ML fully anisotropic, *6* Å Fe layer							1.26
3 ML	Fixed values of 1 ML fully anisotropic, *9* Å Fe layer							1.18

with the surface state being confined to the W(110) interfacial region. The observation that the clean, Fe covered, and Au covered samples all show a similar structure supports the hypothesis that the W(110) interface dominates the anisotropic response.

This feature for the 0, 1, 2 and 3 ML Fe coverage quadrants, capped with Au, can be simulated using a single anisotropic oscillator with different values of $\omega_{0,x}$ and $\omega_{0,y}$ and $\Gamma_x = \Gamma_y$, $A_x = A_y$ (see table 1). Allowing the amplitude and broadening to vary independently produced negligible improvement in the least squares values (χ^2) for the W(110)/Au interface (0 ML patch). The result of the fit is shown in figure 2(b). The RAS shows other, smaller
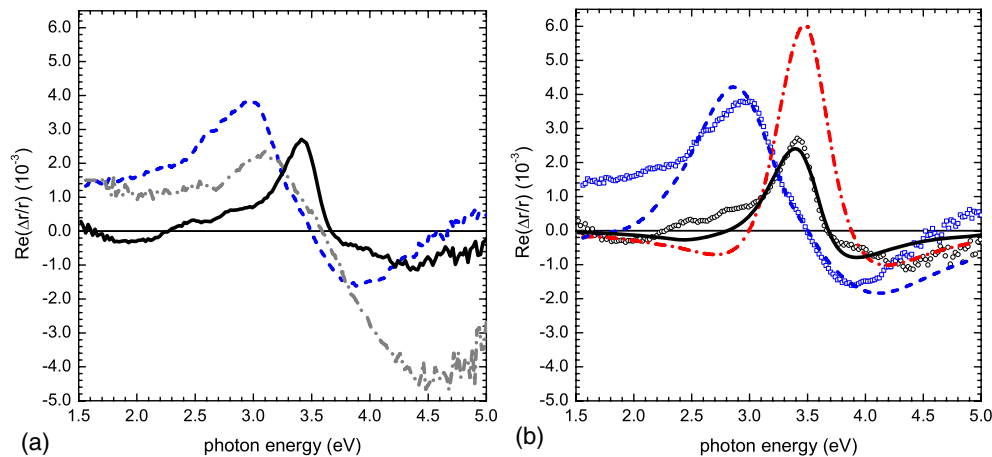
Figure 2. (a) RAS spectra of clean W(110) surfaces and the capped structure: clean, singular W(110) [20] (– – –); clean vicinal W(110) (— · —); vicinal W(110) capped with 16 nm of Au (——). (b) RAS model spectra for the W(110) structures, using equal oscillator strengths: clean, singular W(110) (– – –); vicinal W(110) capped with 16 nm of Au (——); the effect of removing the optically absorbing Au cap in the model (— · —). Data are shown as symbols.

features that will be discussed later. The effect of removing the isotropic Au capping layer from the model structure can now be investigated and figure 2(b) shows the expected increase in amplitude associated with the removal of the optical absorption in the Au layer. A red shift (≈0.4 eV) and broadening ($\Gamma \times 2$) are necessary to simulate the clean surface results of Martin *et al* [20] (figure 2(b)), but the oscillator strength can be left unchanged. These results suggest the same origin for the main RAS feature of the capped structure, with the surface state being blue shifted and sharpened on becoming an interface state, due to the confinement effects of the Fe or Au layers.

The RAS spectra of the sample with 0, 1, 2 and 3 ML Fe coverage are shown in figure 3(a). The 3.4 eV feature changes significantly on Fe adsorption, but shows only a small variation with Fe layer thickness. The results of modelling using the single anisotropic oscillator is shown in figure 3(b). The small differences between the 1, 2, and 3 ML patches can be simply reproduced by using the isotropic bulk dielectric function of Fe. It is not necessary to assume any anisotropic contribution, apart from that of the 3.4 eV feature. For the integer Fe coverages the χ^2 value reduces by a factor of two if the oscillator strength is allowed to be anisotropic ($A_x \neq A_y$). There is always a large error estimate because RAS measures a difference in ε, and oscillator strengths and energetic difference are therefore coupled parameters. Nevertheless, good fits are obtained with a single set of parameters for all the integer Fe layers (see table 1). All the changes in the RAS spectra from 1 to 3 ML Fe can be explained by increasing optical absorption as the isotropic Fe layer increases in thickness, consistent with the main structure originating from the W(110) interface. In addition, the largest variation in figure 3(a) occurs between the 0 and 1 ML patches, as the interface changes from being W(110)/Au to W(110)/Fe, again consistent with main structure originating from this interface. No anisotropic response is detected from the Fe layer, the Fe/Au interface and the Au layer itself. The Fe and Au layers contribute to the measured RAS spectrum only via isotropic optical absorption. Full calculations of the electronic structure of the W(110)/Au and W(110)/Fe interfaces are expected to be the main way that the presence of an anisotropic electronic state localized at the buried W(110) interface will be confirmed: the interfacial region
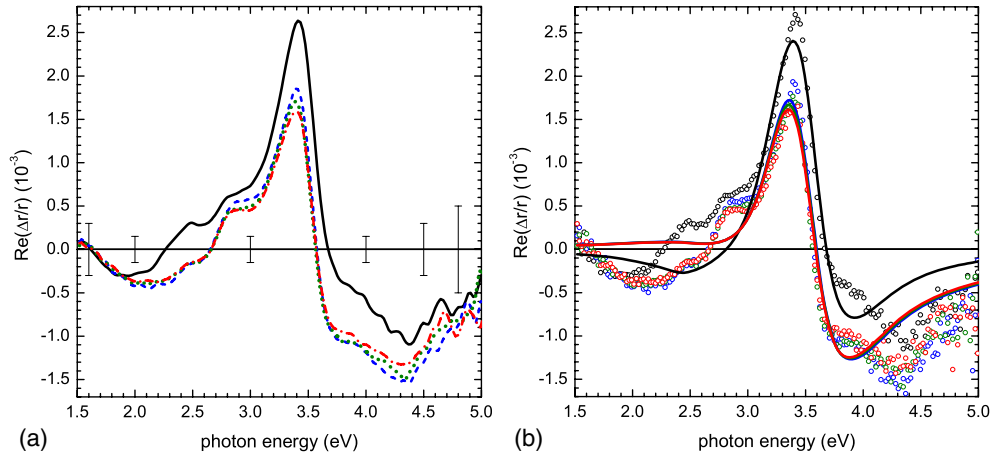
Figure 3. RAS spectra of the vicinal W(110) crystal with integer Fe monolayer coverage and a 16 nm Au capping layer. The 3.4 eV feature changes in amplitude on adsorption of Fe: (a) 0 ML (——), 1 ML (– – –), 2 ML (· · · · · ·), 3 ML (— · —). The original data have been smoothed by convolution with a Gaussian of 0.05 eV width to improve the comparison; (b) least squares fits (solid lines) using a single anisotropic oscillator (raw data shown as symbols).

is inaccessible to electron-based techniques, such as scanning tunnelling spectroscopy or angle-resolved photoemission spectroscopy, that are commonly used to determine the electronic structure of surfaces experimentally.

4. Strain relief and surface roughness

So far, only an anisotropic surface or interface electronic transition has been considered as the origin of the RAS spectra. Other possibilities are uniaxial strain in the interface region, and anisotropic surface or interface roughness. Uniaxial strain in either the bulk tungsten interfacial region or the gold capping layer can lead, in a first order approximation, to small shifts in energy in the electronic structure of the bulk material and hence can be simply simulated by an energetic offset in the dielectric function. This is equivalent to a $\partial \varepsilon / \partial \omega$ shape of the dielectric anisotropy which is frequently found for RAS spectra dominated by modified bulk states [23, 24]. Strain induced RAS has been investigated extensively in semiconductors and can be related to the piezoelectric tensor of the material [25, 26]. For metals, the simple approximation described above has been used successfully to model the anisotropy of other metal surfaces dominated by bulk modifications [27] and this approach will be used here.

Figure 4 shows simulations using a interfacial anisotropy proportional to $\partial \varepsilon / \partial \omega$. A rigid shift of $+0.05$ eV, in ε_x and -0.05 eV in ε_y for the Au capping layer and vice versa for bulk W were used to compare the expected influence of strain to the measured RAS. The thickness of the strained layer was determined by a least square fit to the data. The common feature of strain induced anisotropies is that structures appear at the critical points of the bulk dielectric function.

As can be seen in figure 4 neither of the two possibilities can explain the general shape of the measured RAS spectrum, although the strain model predicts a structure around 3.4 eV for W, indicating that strain at the W(110) interface could contribute to the RAS. The contribution is likely to be small, however, as additional strain induced structures expected at the other W bulk critical points (1.8, 2.4 and 5.2 eV) are not seen. Strain in the Au capping layer produces
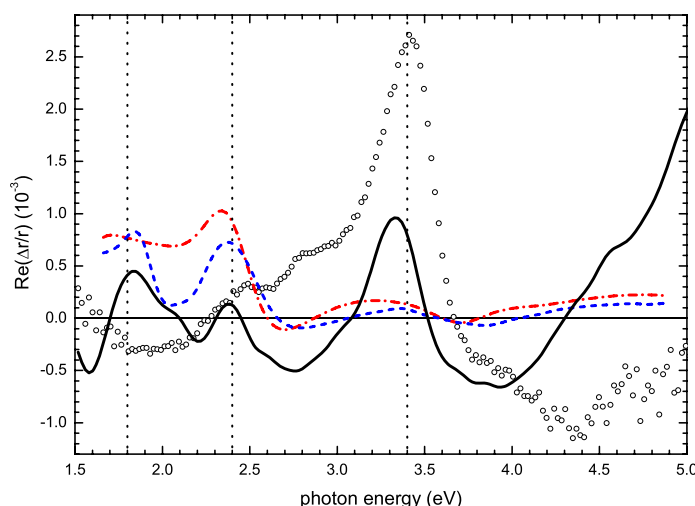
Figure 4. Models of the RAS of uniaxially strained bulk W (——), bulk Au (– – –), and thin film Au (— · —) layers at the interface of the W(110)/Au structure (0 ML patch). The dielectric properties of the strained layers were approximated by a rigid shift of $+0.05$ eV in ε_x and -0.05 eV in ε_y for Au, and vice versa for W. The thickness of the strained layer was derived by a least squares fit. The positions of the bulk critical points of W are marked.

only a much smaller, broad anisotropy around 3.4 eV, indicating that strain in the Au does not contribute to the main peak (the agreement is worse if the bulk Au dielectric function is used). Other bulk dominated effects that give rise to optical anisotropies, such as an anisotropic roughness, can be excluded as contributing to the 3.4 eV feature using the same arguments.

Although uniaxial strain can be excluded as the origin of the main RAS structure, it could contribute to some of the smaller peaks in the RAS spectrum, which are not described by the single oscillator model. Such a contribution would be expected to change with interface composition. Of the smaller peaks, the most significant difference between the patches with and without the Fe monolayers can be seen in figure 3(a) to occur around 2.5 eV (note that normalizing to the 3.4 eV peak height enhances this difference). The changes associated with the formation of the first monolayer, compared to subsequent monolayers, are very different (figure 5). The main change as more Fe is deposited arises from isotropic optical absorption in the Fe layers. The difference, $\delta r/r|_{1-3\ \mathrm{ML}} = \Delta r/r|_{1\ \mathrm{ML}} - \Delta r/r|_{3\ \mathrm{ML}}$, between the 1 and 3 ML Fe patches is shown in figure 5(a), together with the simulated difference obtained by changing only the thickness of the Fe layer in the single oscillator model. Good agreement is obtained, supporting the hypothesis that increasing the thickness of Fe in this coverage regime simply increases the optical absorption of the Fe layers (see figure 3).

Figure 5(b) shows the difference between the 0 and 1 ML patches, together with the oscillator model difference. The data show clearly that there is an unexplained feature at 2.5 eV. The absence of this feature in figure 5(a) is good evidence that it is associated with the formation of the first Fe monolayer and does not change on further deposition.

A possible origin of the 2.5 eV structure is uniaxial strain at the W(110)/Au interface. Detailed studies of RT growth have shown that, by 3 ML coverage, Au has formed a distorted (111) film on singular W(110), with the Au–Au spacing increased along [001] and compressed along [1$\bar{1}$0] [28] while, in contrast, RT growth of Au on singular Fe(110) produces a (111) Au film with a two-dimensional density the same as that of the bulk, thus minimizing strain [29].
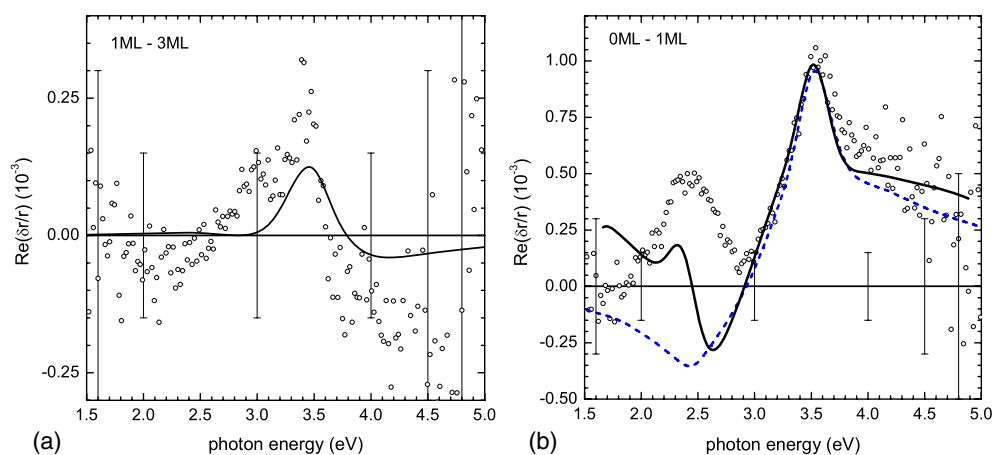
Figure 5. $\delta r/r$ of the 1–3 ML and 0–1 ML patches: (a) $\delta r/r|_{1-3ML}$ can be explained by increased absorption in the Fe layer, as shown by the difference of the modelled spectra (——); (b) $\delta r/r|_{0-1\,ML}$ is compared with the anisotropic oscillator model difference with and without modelled strain relief in the Au capping layer (——, – – – respectively).

In addition, the basic structure of 1, 2 and 3 ML Fe films grown and annealed on W(110) is pseudomorphic monolayer, bilayer and monolayer +Fe(110) islands, respectively [7, 11]. It appears possible, based on these studies, that the interfacial region of the Au film grown on vicinal W(110) will be more strained than that grown on W(110)/Fe. Figure 5(b) shows the simple addition of a scaled strain contribution from the Au capping layer to the anisotropic oscillator model difference. It appears possible that the 2.5 eV structure is related to strain in the Au cap, and that Fe layers sandwiched between the W(110) and Au act to release this strain to a significant extent. Anisotropic roughness of the Au capping layer was also investigated but did not improve the fit significantly, as the main contributions were at higher energies

Summarizing this section, the RAS spectra show a major structure around 3.4 eV that is likely to involve a interface state similar to the surface state found on clean W(110). A smaller structure at 2.5 eV in the RAS spectra may be due to anisotropic strain in the interfacial region of the Au capping layer, which is significantly reduced when intermediate Fe layers are present. The known morphological difference of the 3 ML Fe film (monolayer + islands) has no detectable effect on the RAS response from the capped structures in the investigated spectral region.

5. Submonolayer structures of Fe

For submonolayer coverage of Fe, room temperature deposition followed by annealing produces a monolayer stripe structure, nucleated at the step edges, and with a width dependent on the coverage [7]. Submonolayer coverages of 0.25, 0.5 and 0.75 ML Fe, capped by 12 nm of Au, in four patches were investigated to see whether a contribution from the anisotropic stripes could be identified. The RAS spectra are shown in figure 6(a), and the difference spectra relative to the 0 ML spectrum in figure 6(b). Despite the anisotropic nature of the Fe layer, no substantial difference in the RAS spectrum compared to those of integer monolayers was found. The difference spectra do show, however, that the transition from the 0 to a 1 ML Fe spectrum is not gradual. The 0.25 ML spectrum is similar to the 0 ML spectrum, while the 0.5 ML spectrum already resembles the 1 ML RAS spectrum. If the difference between the
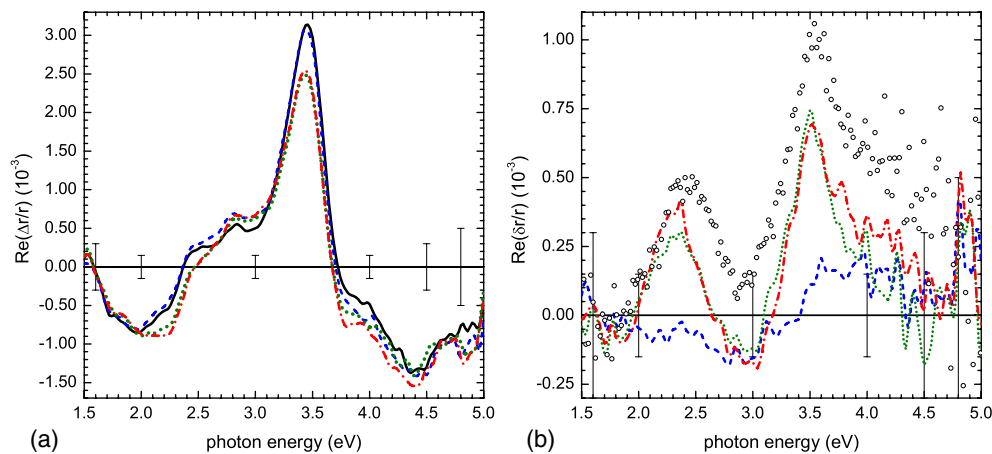
Figure 6. (a) RAS spectra of the vicinal W(110) crystal with 0 (——), 0.25 (– – –), 0.5 (· · · · · ·) and 0.75 ML Fe (— · —) with a 12 nm Au capping layer. The anisotropic nature of the submonolayer Fe structure does not change the RAS spectra significantly. (b) $\delta r/r$ difference spectra relative to the 0 ML patch, compared to the 1 ML difference spectrum (∘). There is an abrupt change between 0.25 and 0.5 ML. All submonolayer spectra have been smoothed by convolution with a Gaussian of 0.05 eV width for clarity.

1 and 0 ML spectrum around 2.5 eV arises from uniaxial interface strain in the Au cap, then 0.5 ML Fe is already significantly reducing that strain. It is interesting that capping with Ag, which has a similar lattice constant to Au, produced RAS spectra that also showed the largest change between 0.25 and 0.5 ML of Fe [13]. A more detailed comparison was not possible for this system, as the Ag caps were not stable in the ambient and the RAS spectra tended to be dominated by contamination and roughness.

6. Long term stability

An intriguing aspect of surface and interface optical techniques is their ability to probe buried and, therefore, protected nanostructures. For the Fe nanostructures it has already been shown that capping with Ag is not sufficient to stabilize the buried Fe nanostructures to exposure to the ambient [13]. Capping with Au has been much more successful. All the measurements shown were performed *ex situ* under ambient conditions either within a few days (submonolayer sample) or within a month (integer monolayer sample) of preparation. In order to investigate long term stability the measurements were repeated for the submonolayer sample 5 months after first air exposure, the sample have been stored under ambient conditions. The RAS amplitudes were smaller by about 25% and the difference spectra show significant changes (figure 7). As RAS is a linear optical technique that measures a difference in reflectance, the reduction in amplitude can be directly correlated to a reduction in anisotropic interface area. The RAS results show that, after 5 month of air exposure, 75% of the interface area is intact. Whether the same holds true for the Fe structure itself cannot be determined, as the submonolayer Fe structures do not produce a RAS signature.

The second obvious change is a reduction in the additional structure at 2.5 eV for the aged sample, shown in the $\delta r/r$ spectra in the figure. If this structure arises from interfacial strain, then this is being reduced by the migration of contamination into the interfacial region of the Au layer during prolonged exposure to the ambient.
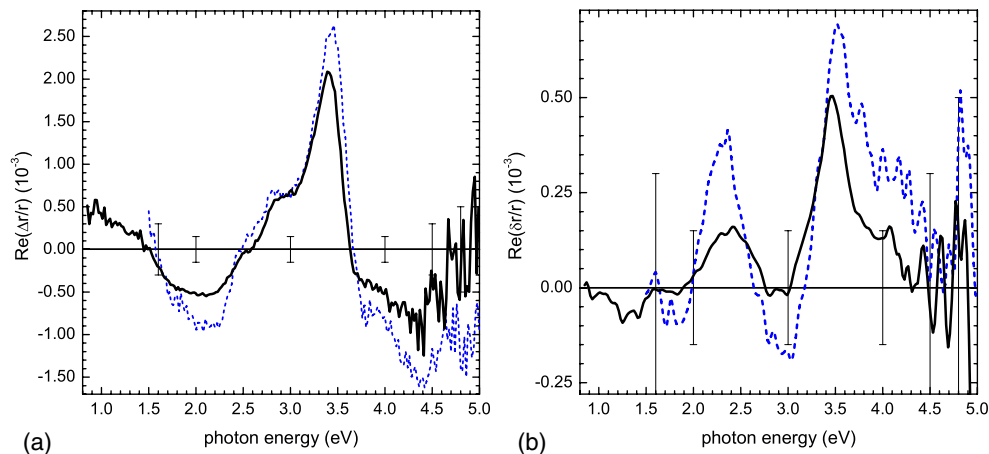
Figure 7. (a) RAS spectra of the 0.75 ML patch with 12 nm capping layer after preparation (– – –) and after 5 month air exposure (——). (b) RAS difference spectra, $\delta r/r|_{0-0.75\ \text{ML}}$, again after preparation and 5 months later. The difference spectra have been smoothed by convolution with a Gaussian of 0.05 eV width for clarity.

7. Conclusions

RAS has been used to show that thin capping layers of Au can protect the Fe/W(110) interface from exposure to the ambient for several months. The main feature in the RAS response was attributed to transitions in the band structure involving a interface state closely related to the surface state found on clean W(110) surfaces, while a smaller feature was attributed to anisotropy in the capping layer response introduced by uniaxial interface strain. The difference between spectra with and without Fe layers was consistent with expected changes in the interfacial strain arising from the different Fe and Au lattice constants. However *ex situ* RAS is shown not to be useful in this particular system to investigate the properties of the submonolayer Fe nanostructures itself, as no anisotropic signature was found other than that assigned to strain relief between 0.25 and 0.5 ML Fe coverage.

Acknowledgments

References

[1]　McGilp J F 1995 *Prog. Surf. Sci.* **49** 1
[2]　Kirilyuk A and Rasing T 2005 *J. Opt. Soc. Am.* B **22** 148
[3]　Sander D 2004 *J. Phys.: Condens. Matter* **16** 603
[4]　Przybylski M and Gradmann U 1987 *Phys. Rev. Lett.* **59** 1152
[5]　Elmers H, Liu G and Gradmann U 1989 *Phys. Rev. Lett.* **63** 566
[6]　Hauschild J, Elmers H J and Gradmann U 1998 *Phys. Rev.* B **57** R677
[7]　Elmers H J, Hauschild J and Gradmann U 1999 *Phys. Rev.* B **59** 3688
[8]　Elmers H, Hauschild J and Gradmann U 2000 *J. Magn. Magn. Mater.* **221** 219

 [9] Pratzer M and Elmers H 2002 *Phys. Rev.* B **66** 033402
[10] Pratzer M and Elmers H 2003 *Phys. Rev.* B **67** 94416
[11] Bode M, Wachowiak A, Wiebe J, Kubetzka A, Morgenstern M and Wiesendanger R 2004 *Appl. Phys. Lett.*
        84 948
[12] Carroll L and McGilp J F 2007 at press
[13] Carroll L, Pedreschi F, O'Mahony J D and McGilp J F 2005 *Phys. Status Solidi* b **242** 2650
[14] Kooij E S, Wormeester H, Brouwer E A M, van Vroonhoven E, van Silfhout A and Poelsema B 2002 *Langmuir*
        18 4401
[15] Aspnes D E, Harbison J P, Studna A A and Florez L T 1988 *J. Vac. Sci. Technol.* A **6** 1327
[16] Weightman P, Martin D S, Cole R J and Farrell T 2005 *Rep. Prog. Phys.* **68** 1251
[17] Palik E D 1985 *Handbook of Optical Constants of Solids* (New York: Academic)
[18] Hunderi O, Zettler J T and Haberland K 2005 *Thin Solid Films* **472** 261
[19] Johnson P B and Christy R W 1974 *Phys. Rev.* B **9** 5056
[20] Martin D, Zeybek O, Sheridan B, Barrett S, Weightman P, Inglesfield J and Crampin S 2001 *J. Phys.: Condens.
        Matter* **13** 607
[21] Baumberger F, Herrmann T, Kara A, Stolbov S, Esser N, Rahman T, Osterwalder J, Richter W and Greber T 2003
        Phys. Rev. Lett. **90** 177402
[22] Sheridan B, Martin D, Power J, Barrett S, Smith L, Lucas C, Nichols R and Weightman P 2000 *Phys. Rev. Lett.*
        85 4618
[23] Mantese L, Rossow U and Aspnes D E 1996 *Appl. Surf. Sci.* **107** 35
[24] Rossow U, Mantese L and Aspnes D E 1998 *Appl. Surf. Sci.* **123** 237
[25] Hingerl K, Balderas-Navarro R E, Bonanni A, Tichopadek P and Schmidt W G 2001 *Appl. Surf. Sci.* **175** 769
[26] Papadimitriou D and Richter W 2005 *Phys. Rev.* B **72** 075212
[27] Martin D S, Cole R J and Weightman P 2005 *Phys. Rev.* B **72** 035408
[28] Bauer R S, Bachrach R Z, McMenamin J C and Aspnes D E 1977 *Nuovo Cimento* B **39** 409
[29] Elmers H and Gradmann U 1994 *Surf. Sci.* **304** 201